NJC

Syntheses, structural characterizations and biological activities of spiro-ansa-spiro-cyclotriphosphazenes

Journal:	*New Journal of Chemistry*
Manuscript ID:	NJ-ART-06-2015-001530.R1
Article Type:	Paper
Date Submitted by the Author:	17-Aug-2015
Complete List of Authors:	Başterzi, Nisan; Ankara University, Department of Chemistry Bilge Koçak, Selen; Ankara University, Department of Chemistry Okumuş, Aytuğ; Ankara University, Department of Chemistry Kılıç, Zeynel; Ankara University, Department of Chemistry Hökelek, Tuncer; Hacettepe University, Department of Physics Çelik, Ömer; Dicle University, Department of Physics Turk, Mustafa; Kırıkkale University, Department of Bioengineering Koç, Lütfiye; The Turkish Sugar Authority, Açık, Leyla; Gazi University, Aydın, Betül; Gazi University, biology

Syntheses, structural characterizations and biological activities of *spiro-ansa-spiro*-cyclotriphosphazenes

Nisan Sevin Başterzi · Selen Bilge Koçak · Aytuğ Okumuş · Zeynel Kılıç · Tuncer Hökelek · Ömer Çelik · Mustafa Türk · L. Yasemin Koç · Leyla Açık · Betül Aydın

Nisan Sevin Başterzi · Selen Bilge Koçak(✉) · Aytuğ Okumuş · Zeynel Kılıç

Department of Chemistry
Ankara University
06100 Tandoğan-Ankara, Turkey
Phone: +90-312-2126720
Fax: +90-312-2232395
E-mail: sbilge@science.ankara.edu.tr

Tuncer Hökelek

Department of Physics
Hacettepe University
06800 Beytepe-Ankara, Turkey

Ömer Çelik

Department of Physics
Dicle University
21280 Sur-Diyarbakır, Turkey

Mustafa Türk

Department of Bioengineering
Kırıkkale University
71450 Yahşihan-Kırıkkale, Turkey

L. Yasemin Koç · Leyla Açık · Betül Aydın

Department of Biology
Gazi University
06500 Beşevler-Ankara, Turkey

Syntheses, structural characterizations and biological activities of *spiro-ansa-spiro*-cyclotriphosphazenes

Nisan Sevin Başterzi,[a] Selen Bilge Koçak,*[a] Aytuğ Okumuş,[a] Zeynel Kılıç,[a] Tuncer Hökelek,[b] Ömer Çelik,[c] Mustafa Türk,[d] L. Yasemin Koç,[e] Leyla Açık[e] and Betül Aydın[e]

[a] *Department of Chemistry, Ankara University, 06100 Tandoğan-Ankara, Turkey*

[b] *Department of Physics, Hacettepe University, 06800 Beytepe-Ankara, Turkey*

[c] *Department of Physics, Dicle University, 21280 Sur-Diyarbakır, Turkey*

[d] *Department of Bioengineering, Kırıkkale University, 71450 Yahşihan-Kırıkkale, Turkey*

[e] *Department of Biology, Gazi University, 06500 Beşevler-Ankara, Turkey*

Abstract

The replacement reactions of the Cl–atoms in partly substituted *spiro-ansa-spiro*-cyclotriphosphazenes (**7** and **8**) with excess pyrrolidine, 4-(2-aminoethyl)morpholine, and 1,4-dioxa-8-azaspiro[4,5]decane in dry THF led to the formation of the heterocyclic amine substituted cyclotriphosphazenes (**9a**–**c** and **10a**–**c**). All cyclotriphosphazene derivatives were characterized by elemental analysis, FTIR, MS, 1D ^{1}H, ^{13}C and ^{31}P NMR and 2D HSQC, and HMBC techniques, and the crystal structure of partly substituted cyclotriphosphazene **8** was verified by X-ray diffraction analysis. The cyclotriphosphazene derivatives (**5**–**8**, **9a**–**c**, and **10a**–**c**) were subjected to antimicrobial activity against seven clinic bacteria and one yeast strain, and the interactions of the phosphazenes with plasmid pBR322 DNA were investigated. Phosphazene derivatives [(**5**, **7**, **8**, **9b** and **9c**) and (**10a** and **10b**)] caused a slight increase and substantial decrease in the mobility of form I DNA, respectively, while **9a** caused retardation on gel. The evaluations of cytotoxic, apoptotic and necrotic effects against L929 fibroblast and A549 lung cancer cells were also studied. While the highest toxic effect was obtained for **9a** in L929 fibroblast cells and for **9c** in A549 lung cancer cells at 100 µg/mL concentration, the highest apoptotic effect was determined for **10a** in L929 fibroblast cells and for **9a** in A549 lung cancer cells at the same concentration. It was found that **9a** and **10b** exhibited the most necrotic effects against L929 fibroblast and A549 lung cancer cells, respectively. The toxic and necrotic effects of the phosphazenes against A549 lung cancer cells were greater than those against L929 fibroblast cells, whereas, the apoptotic effect of the compounds was greater in L929 fibroblast cells than in A549 lung cancer cells.

Keywords: *spiro-ansa-spiro*-cyclotriphosphazenes, spectroscopy, DNA interactions, cytotoxicity, apoptotic and necrotic effects

* Corresponding author. Tel.: +90 312 2126720-1021; fax: +90 312 2232395.
E-mail address: sbilge@science.ankara.edu.tr (S. Bilge Koçak).

1. Introduction

The term ''*cyclophosphazenes*'' refers to a prominent family of heterocyclic rings with an inorganic backbone containing the repeating unit $[NPR_2]_n$ (n=3, 4, 5, …), and two organic, inorganic, and organometallic side groups (R), attached to each P–atom.[1] Among this family of compounds, hexachlorocyclotriphosphazene (cyclic trimer, $N_3P_3Cl_6$) has received particular attention in phosphazene-based chemistry. This interest mostly arises from the replacement reactions of highly reactive Cl–atoms of $N_3P_3Cl_6$ with various nucleophilic reagents for the preparation of a wide range of phosphazene derivatives with diverse applications of technological and medicinal importance;[2] (e.g., ionic liquids,[3] liquid crystals,[4] flame-retardant additives to organic polymers,[5] light-emitting diodes,[6] and electrolytes for lithium-ion batteries.[7] Numerous cyclotriphosphazenes have been synthesized with –NH or –OH functioned nucleophilic reagents, including primary and secondary amines,[8,9] polyamines,[10] and phenoxides.[11,12] At the same time, investigations of replacement reaction patterns of Cl–atoms in $N_3P_3Cl_6$ with difunctional nucleophiles have recently attracted the interest of many scientists due to the formation of numerous structural isomers and stereoisomers, (e.g., *spiro*-, *ansa*-, or *bino*-products).[13,14] These reactions especially depend on the chain lengths of the reacting functional groups, the reaction temperature, and the solvent polarities.[15] In fact, the number of *spiro-ansa* cyclotriphosphazenes remains limited in relevant literature.[16–18]

Cancer is a growing health problem around the world. Lung cancer especially is the second most common cancer in men after liver cancer, is the most frequent cause of cancer-related death, and accounts for more than one million deaths yearly worldwide. While naturally occurring compounds have long been used to cure many types of cancer, a great deal of research is currently being performed to design new compounds for the development of anticancer drugs. As known, mono- and poly amino-substituted cyclotriphosphazenes pose potential value in cancer therapies,[19–24] given their cytotoxic activities on the human colon carcinoma (HT-29), human laryngeal epidermoid carcinoma (Hep2), and African green monkey kidney (Vero) cells, as well as their ability to induce apoptosis.[25] Moreover, the antimicrobial activity of cyclotriphosphazenes against various bacteria and fungi has been observed.[26,27] Our research team is interested in the reactions of N_2O_2-donor type tetradentate symmetric ligands with $N_3P_3Cl_6$ for the purposes of obtaining *spiro-ansa-spiro*- (**sas**) and *spiro-bino-spiro*- (**sbs**) products and of exploring their biological activities and interactions with DNA. In continuation of our research on

syntheses and structures of **sas** and **sbs** cyclotriphosphazene derivatives, the present study focused primarily on the synthesis and structural determination of cyclotriphosphazene compounds, with the aim of introducing the heterocyclic amine groups pyrrolidine, 4-(2-aminoethyl)morpholine (AEM) and 1,4-dioxa-8-azaspiro[4,5]decane (DASD) to partly substituted **sas** phosphazenes (Scheme 1). We also sought to investigate their DNA binding, *in vitro* antimicrobial activities, and cytotoxic, apoptotic, and necrotic effects upon L929 fibroblast and A549 lung cancer cells. Characterizations of the new cyclotriphosphazenes (**9b**, **9c** and **10a**–**c**) were carried out by elemental analysis, electrospray ionization mass spectrometry (ESI-MS), Fourier transform infrared (FTIR), one-dimensional (1D) ^{1}H, ^{13}C, and ^{31}P NMR, two-dimensional (2D) heteronuclear single-quantum correlation (HSQC), and heteronuclear multiple-bond correlation (HMBC) techniques. The crystal structure of partly substituted **sas 8** phosphazene was also determined using X-ray crystallography.

2. Experimental

2.1. Materials used for synthesis

Commercial grade reagents were used without further purification, and solvents were dried and distilled by standard methods. The solvents, salicylaldehyde, sodium borohydride, borax and potassium carbonate were purchased from Merck, while aliphatic amines, pyrrolidine, AEM, and DASD were purchased from Fluka. Hexachlorocyclotriphosphazene, $N_3P_3Cl_6$ (Fluka) was purified by fractional crystallization from *n*-hexane, and all reactions were monitored using thin-layer chromatography (TLC) on Merck DC Alufolien Kieselgel 60 B_{254} sheets. Column chromatography was performed on Merck Kieselgel 60 (230-400 mesh ATSM) silica gel, and all reactions were conducted in an argon atmosphere.

2.2. Physical measurements

Melting points were measured with a Gallenkamp apparatus using a capillary tube. Microanalyses (C, H, N) were performed using Leco CHNS-932 elemental analyzer at the Central Instrumental Analysis Laboratory in the Faculty of Pharmacy at Ankara University. ^{1}H (400 MHz) and ^{13}C (100 MHz)

NMR, HSQC, and HMBC spectra were recorded employing a Varian Mercury 400 MHz FT spectrometer, while ^{31}P NMR spectra were obtained by using a Bruker DPX FT-NMR 500 MHz spectrometer; $SiMe_4$ was used as an internal standard for ^{1}H and ^{13}C NMR and external 85% H_3PO_4 for ^{31}P NMR. IR spectra were recorded on a Mattson 1000 FTIR spectrometer using KBr pellets. ESI-MS mass spectra were obtained on an Agilent 1100 MSD spectrometer.

2.3. Syntheses

*2.3.1. Syntheses of the compounds (**1**–**8** and **9a**)*

Dibenzo-*bis*-imino-podands {N,N´-bis(salicylidene)-1,3-propanediamine (**1**) and N,N´-bis(salicylidene)-1,4-butanediamine (**2**)} were prepared according to the published procedure in which salicylaldehyde was reacted with 1,3-diaminopropane and 1,4-diaminobutane in dry MeOH, respectively.[28] Dibenzo-diaza podands {bis[N,N'-(2-hydroxybenzyl)]1,3-diaminopropane (**3**) and bis[N,N'-(2-hydroxybenzyl)]1,4-diaminobutane (**4**)} were synthesized from the reduction of **1** and **2** with $NaBH_4/Na_2B_4O_7.10H_2O$ in dry MeOH, respectively.[28] The partly substituted **sbs** phosphazenes {3,3″-propane-1,3-diylbis[4´,4´,6´,6´-tetrachloro-3,4-dihydrospiro[1,3,2-benzoxazaphosphorine-2,2´λ^5-[4λ^5,6λ^5][1,3,5,2,4,6] triazatriphosphorine]] (**5**) and 3,3″-butane-1,4-diylbis[4´,4´,6´,6´-tetrachloro-3,4-dihydrospiro [1,3,2-benzoxazaphosphorine-2,2´λ^5-[4λ^5,6λ^5][1,3,5,2,4,6]triazatriphosphorine]] (**6**)} and **sas** phosphazenes {*meso*-8,8-dichloro-18,19,20-trihydro-6λ^5,8λ^5,10λ^5-6,10-nitrilo-16*H*,22*H*[1,3,5,7,2,4,6] tetrazatriphosphecino[2,1-b:6,7-b′]bis[1,3,2]benzoxazaphosphorine (**7**) and *meso*-8,8-dichloro-18,19,20,21-tetraydro-6λ^5,8λ^5,10λ^5-6,10-nitrilo-16*H*,23*H*[1,3,5,7,2,4,6]tetrazatriphosphecino[2,1-b:6,7-b′] bis[1,3,2]benzoxazaphosphorine (**8**)} were prepared using a method in which dibenzo-diaza-podands (**3** and **4**) and $N_3P_3Cl_6$ were refluxed in dry THF according to the published procedure by our research group.[29,30] The preparation and spectroscopic data of fully pyrrolidine substituted **sas** phosphazene {*meso*-8,8-18,19,20-trihydro-8,8-dipyrrolidine-1-yl-6λ^5,8λ^5,10λ^5-6,10-nitrilo-16*H*,22*H*[1,3,5,7,2,4,6] tetrazatriphosphecino[2,1-b:6,7-b′]bis[1,3,2]benzoxazaphosphorine} (**9a**) was reported by our group[30] but, antimicrobial activities and DNA interaction studies of **5**–**8** and **9a** were discussed in this paper for comparison purposes.

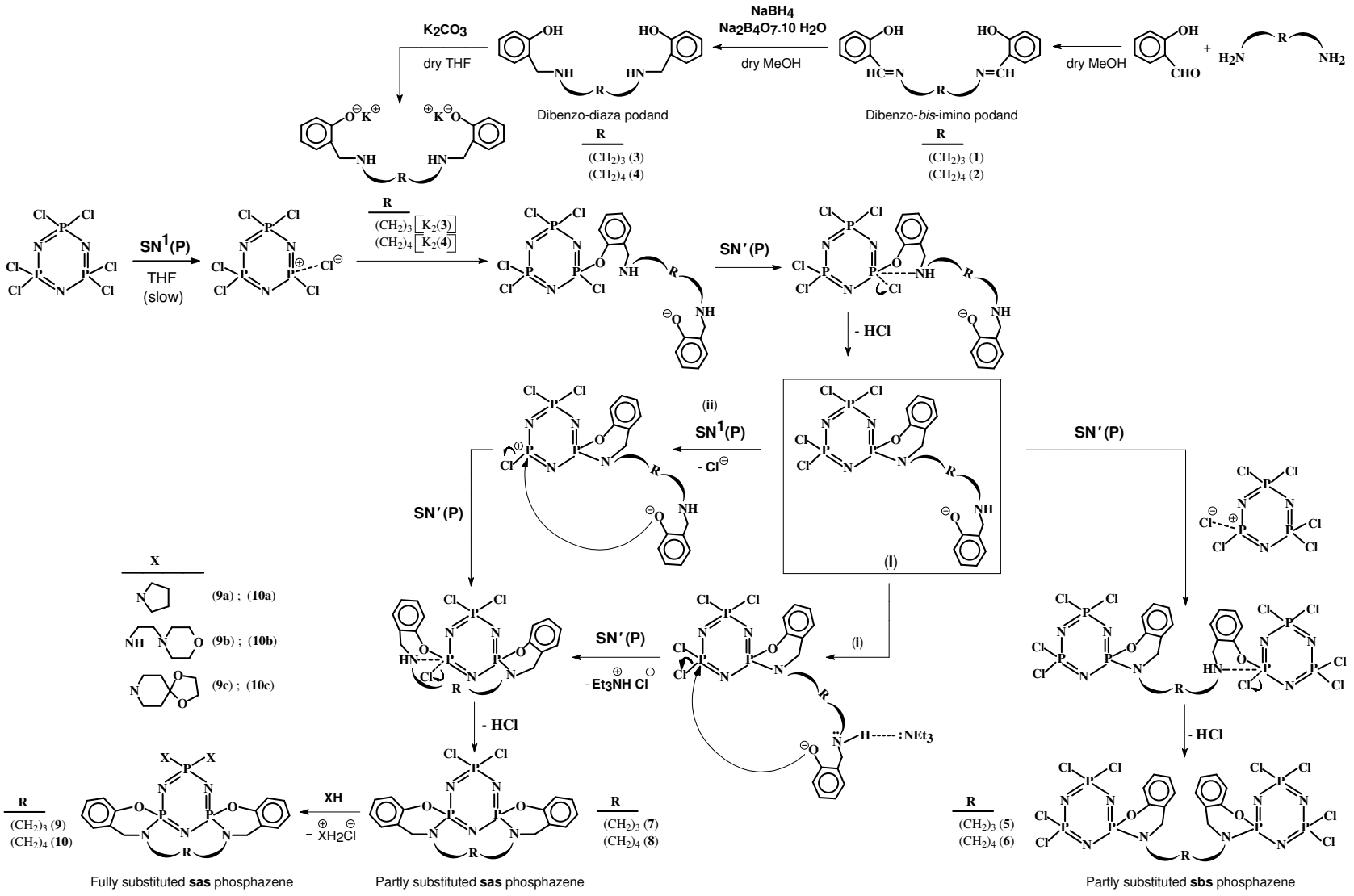

Scheme 1 Reaction pathways of $N_3P_3Cl_6$ with dibenzo-diaza podands (**3** and **4**) and **sas** (**9a**–**c** and **10a**–**c**) phosphazenes obtained from the reactions of **sas** (**7** and **8**) with pyrrolidine, AEM, and DASD.

*2.3.2. Syntheses of the new compounds (**9b**, **9c** and **10a–c**)*

Fully substituted **sas** phosphazenes (**9b**, **9c** and **10a–c**) were prepared by similar methods; therefore, the experimental procedure of the preparation was only described in detail for the first case.

*2.3.2.1. meso-18,19,20-Trihydro-8,8-di[4-(2-aminoethyl)morpholine]-1-yl-6λ^5,8λ^5,10λ^5-6,10-nitrilo-16H,22H[1,3,5,7,2,4,6]tetrazatriphosphecino[2,1-b:6,7-b']bis[1,3,2]benzoxazaphosphorine (**9b**)*

A solution of AEM (0.95 g, 7.30 mmol) in dry THF (30 mL) was slowly added to a stirred solution of **7** (0.60 g, 1.20 mmol) in dry THF (150 mL) at room temperature. The mixture was stirred for 60 h at room temperature under argon and followed by TLC indicating no starting material remaining. The precipitated AEM hydrochloride was filtered off, and the solvent was evaporated. The crude product was subjected to column chromatography [silica gel 60 (230-400 mesh) (15 g) as adsorbent and THF as the eluent, R_f=0.20] and crystallized from CH_3CN. Yield: 0.55 g (67 %). mp: 66 ^oC. Anal. Calc. for $C_{29}H_{42}N_9O_4P_3$ (%): C, 51.55; H, 6.56; N, 18.65. Found: C, 51.19; H, 6.59; N, 18.55. IR (KBr, cm^{-1}): ν 3321 (N-H), 3045 (C-H arom.), 2953-2854 (C-H aliph.), 1587 (C=C), 1178 (P=N), 1152 (C-O). ESI-MS (I_r %): *m*/*z* 676 {[*M*H]$^+$, 100}, 547 {[*M*H-AEM]$^+$, 17}, 418 {[*M*H-2AEM]$^+$, 7}.

*2.3.2.2. meso-18,19,20-Trihydro-8,8-di[1,4-dioxa-8-azaspiro[4,5]decane]-1-yl-6λ^5,8λ^5,10λ^5-6,10-nitrilo-16H,22H[1,3,5,7,2,4,6]tetrazatriphosphecino[2,1-b:6,7-b']bis[1,3,2]benzoxazaphosphorine (**9c**)*

Compound (**9c**) was prepared from DASD (1.74 g, 12.2 mmol) and **7** (1.00 g, 2.00 mmol) (21 h), column chromatography [silica gel (15 g), benzene, R_f=0.63], crystallized from CH_3CN. Yield: 0.60 g (41 %). mp: 190 ^oC. Anal. Calc. for $C_{31}H_{42}N_7O_6P_3$ (%): C, 53.07; H, 6.03; N, 13.97. Found: C, 53.25; H, 5.97; N, 13.86. IR (KBr, cm^{-1}): ν 3061 (C-H arom.), 2956-2830 (C-H aliph.), 1585 (C=C), 1192 (P=N), 1155 (C-O). ESI-MS (I_r %): *m*/*z* 702 {[*M*H]$^+$, 100}, 560 {[*M*H-DASD]$^+$, 13}.

*2.3.2.3. meso-18,19,20,21-Tetrahydro-8,8-dipyrrolidine-1-yl-6λ^5,8λ^5,10λ^5-6,10-nitrilo-16H,23H [1,3,5,7,2,4,6]tetrazatriphosphecino[2,1-b:6,7-b']bis[1,3,2]benzoxazaphosphorine (**10a**)*

Compound (**10a**) was prepared from pyrrolidine (0.59 g, 8.40 mmol) and **8** (0.70 g, 1.40 mmol) (29 h), column chromatography [silica gel (15 g), benzene/THF (5/1), R_f=0.44], crystallized from CH_2Cl_2/*n*-hexane (5/1). Yield: 0.42 g (73 %). mp: 167 ^oC. Anal. Calc. for $C_{26}H_{36}N_7O_6P_3$ (%): C, 54.64; H, 6.35; N,

17.15. Found: C, 54.56; H, 6.43; N, 17.03. IR (KBr, cm^{-1}): ν 3070 (C-H arom.), 2958-2866 (C-H aliph.), 1585 (C=C), 1174 (P=N). ESI-MS (I_r %): *m*/*z* 572 {[*M*H]$^+$, 100}, 502 {[*M*H-pyr]$^+$, 2}.

*2.3.2.4. meso-18,19,20,21-Tetrahydro-8,8-di[4-(2-aminoethyl)morpholine]-1-yl-6λ^5,8λ^5,10λ^5-6,10-nitrilo-16H,23H[1,3,5,7,2,4,6]tetrazatriphosphecino[2,1-b:6,7-b']bis[1,3,2]benzoxazaphosphorine (**10b**)*

Compound (**10b**) was prepared from AEM (0.77 g, 6.00 mmol) and **8** (0.50 g, 1.00 mmol) (64 h), column chromatography [silica gel (15 g), THF, R_f=0.20], crystallized from CH_2Cl_2. Yield: 0.35 g (51 %). mp: 67 ^{o}C. Anal. Calc. for $C_{30}H_{46}N_9O_4P_3$ (%): C, 52.28; H, 6.71; N, 18.25. Found: C, 51.71; H, 6.34; N, 18.35. IR (KBr, cm^{-1}): ν 3336 (N-H), 3062 (C-H arom.), 2954-2856 (C-H aliph.), 1587 (C=C), 1171 (P=N), 1115 (C-O). ESI-MS (I_r %): *m*/*z* 690 {[*M*H]$^+$, 100}, 561 {[*M*H-AEM]$^+$, 15}, 432 {[*M*H-2AEM]$^+$, 3}.

*2.3.2.5. meso-18,19,20,21-Tetrahydro-8,8-di[1,4-dioxa-8-azaspiro[4,5]decane]-1-yl-6λ^5,8λ^5,10λ^5-6,10-nitrilo-16H,23H[1,3,5,7,2,4,6]tetrazatriphosphecino[2,1-b:6,7-b']bis[1,3,2]benzoxazaphosphorine (**10c**)*

Compound (**10c**) was prepared from DASD (0.85 g, 5.94 mmol) and **8** (0.50 g, 1.00 mmol) (40 h), column chromatography [silica gel (15 g), benzene/THF (3/1), R_f=0.62], crystallized from CH_2Cl_2/*n*-hexane (5/1). Yield: 0.42 g (54 %). mp: 196 ^{o}C. Anal. Calc. for $C_{32}H_{44}N_7O_6P_3$ (%): C, 53.72; H, 6.20; N, 13.71. Found: C, 54.01; H, 6.63; N, 13.23. IR (KBr, cm^{-1}): ν 3066 (C-H arom.), 2926-2864 (C-H aliph.), 1585 (C=C), 1211 (asymm.), 1173 (symm.) (P=N), 1150 (C-O). ESI-MS (I_r %): *m*/*z* 716 {[*M*H]$^+$, 100}.

2.4. Single crystal X-ray structure determination

The colorless crystals of compound **8** were crystallized from benzene. Detailed crystallographic data and structure refinement parameters appear in Table 1,[31,32] while selected bond lengths and angles appear in Table 2. Crystallographic data were recorded in a Bruker Breeze APEXII CCD area-detector diffractometer using Mo K_α radiation (λ=0.71073 Å) at T=294 K. Absorption corrections by multi-scan[33] were applied. Structures were solved by direct methods and refined by full-matrix least squares against F^2 using all data.[34] All non-H atoms were refined anisotropically. Aromatic and methylene H atoms were positioned geometrically at distances of 0.93 (CH) Å and 0.97 (CH_2) Å from the parent C atoms, and a riding model was used during the refinement process. U_{iso}(H) values were constrained to 1.2U_{eq} for methine and methylene carrier atoms.

Table 1 Crystallographic data for **8**

Empirical formula	$C_{18}H_{20}Cl_2N_5O_2P_3 \cdot C_6H_6$
Color/shape	Colorless / block
Formula weight	580.31
Temperature (K)	294(2)
Radiation used, graphite monochromator	MoK_α (λ = 0.71073 Å)
Crystal system	P –1
Space group	Triclinic
a, b, c (Å)	9.6261(3), 10.9469(3), 14.6288(4)
α, β, γ (º)	72.336(3), 89.163(3), 65.679(2)
V ($Å^3$)	1327.63(7)
Z	2
Absorption coefficient (mm^{-1})	0.458
D_{calc} (Mg m^{-3})	1.452
Max. Crystal dimen. (mm)	0.10 × 0.15 × 0.25
θ (max) (^{o})	27.65
Reflections measured	4770
Range of *h*, *k*, *l*	$-12 < h < 9$; $-14 < k < 3$; $-18 < l < 15$
Diffractometer/scan	Bruker Breeze APEXII CCD/ *φ* and *w*
Number of reflections with I >2 σ(I)	3494
Corrections applied	Lorentz-polarization
Computer programs	SHELXS97, SHELXL97, ORTEP-3, PLATON
Source of atomic scattering factors	Int. Table for X-ray Cryst. Vol. IV, 1974
Structure solution	Direct methods
Treatment of hydrogen atoms	Geometric calculations
No. of parameters var.	325
GOF	1.036
$R = \|\|F_o\| - \|F_c\|\|/\|F_o\|$	0.0634
R_w	0.1297
$(\Delta/\rho)_{max}$ (eA^{-3})	0.368
$(\Delta/\rho)_{min}$ (eA^{-3})	–0.267

Table 2 Selected bond lengths (Å) and angles (º) for **8**

P1–Cl1	2.0147(14)	P2–N2	1.579(3)
P1–Cl2	2.0169(14)	P2–N5	1.631(3)
P1–N1	1.560(3)	P3–O1	1.590(3)
P1–N3	1.570(3)	P3–N2	1.570(3)
P2–O2	1.578(2)	P3–N3	1.605(3)
P2–N1	1.603(3)	P3–N4	1.641(3)
C7–N4–C8	117.3(4)	N2–P3–N3	113.61(15)
P1–N4–C7	120.8(3)	N1–P2–N2	114.60(15)
P3–N4–C8	116.1(3)	P1–N1–P2	120.14(17)
C11–N5–C12	116.1(3)	P2–N2–P3	125.41(19)
P2–N5–C11	120.9(3)	Cl1–P1–Cl2	98.91(7)
P2–N5–C12	120.9(3)	O1–P3–N4	102.53(16)
N1–P1–N3	121.21(16)	O2–P2–N5	102.89(14)
P1–N3–P3	120.97(18)	C8–C9–C10	116.0(5)

2.5. Evaluation of in vitro antimicrobial activity

Antimicrobial susceptibility experiments were performed using the agar well-diffusion method with a minor modification.[35] The organisms used in antimicrobial screening included seven bacteria namely, *Staphylococcus aureus* ATCC 25923 (G+), *Bacillus subtilis* ATCC 6633 (G+), *Bacillus cereus* NRRL-B-3711 (G+), *Enterococcus faecalis* ATCC 292112 (G+)*, Pseudomonas aeruginosa* ATCC 27853 (G–), *Escherichia coli* ATCC 25922 (G–) and *Escherichia coli* ATCC 35218 (G–) and the fungus *Candida albicans* ATCC 10231. The test compounds were dissolved in 1,4-dioxane, after which gram-negative and gram-positive bacteria were grown on Müller-Hinton agar medium and incubated at 37 ºC for 24 h. The yeast strain was grown in Sabouraud dextrose agar and incubated at 30 ºC for 48 h. A suspension of the tested microorganism (0.1 mL of 10^8 cells/mL) was spread over the surface of the agar plates, wells with 8.0 mm diameters were cut into the medium, and 50 µL test compound (5000 µM) was added to each well. Before incubation, all Petri dishes were refrigerated (4 ºC) for 2 h. After incubation, the diameter of the inhibition zone was measured in millimeters. All experiments were repeated three times; the mean values are presented. *Ampicillin* (10 µg) and *Chloramphenicol* (30 µg) were used as standard antibacterial agents, while *Ketoconazole* (50 µg) was used as an antifungal control.

2.6. DNA cleavage activity

The interactions of $N_3P_3Cl_6$, pyrrolidine, AEM, DASD, dibenzo-diaza podands (**3** and **4**), **sbs** (**5** and **6**), and **sas** (**7**, **8**, **9a**–**c**, and **10a**–**c**) cyclotriphosphazenes with pBR322 plasmid DNA were studied, and the screenings of DNA–compound interactions were carried out via electrophoresis on a 1% agarose gel.[36] The compounds were dissolved in 1,4-dioxane, and the solutions of the compounds were immediately applied to the plasmid DNA. The plasmid DNA aliquots were incubated in the presence of increasing concentrations of the compounds ranging from 312 µM to 5000 µM at 37 ºC for 24 h in the dark. Ten µL aliquots of compound/DNA mixtures were loaded onto the 1% agarose gel with a loading buffer (0.1% bromophenol blue, 0.1% xylene cyanol), and electrophoresis was performed in 0.05 M Tris base, 0.05 M glacial acetic acid and 1 mM EDTA (TAE buffer, pH = 8.0) for 3 h at 80V.[37] Later, the gel was stained with ethidium bromide (0.5 µg/mL), visualized under UV light using a transilluminator (BioDoc Analyzer, Biometra), photographed with a video-camera, and saved as a TIFF file. The experiments were repeated three times. Untreated Supercoiled DNA was used as a control.

2.7. Determination of cytotoxicity with WST-1

A549 lung cancer cells were obtained from the Division of Biochemistry of the Medicinal Science Faculty at Uludağ University (Bursa, Turkey), and L929 fibroblast cell lines were supplied by the ŞAP Institute of Ministry of Agriculture (Ankara, Turkey). Cell culture flasks and other plastic materials were purchased from Corning (New York, USA). The growth medium, Dulbecco's modified eagle medium (DMEM) without L-glutamine supplemented with fetal calf serum (FCS) and trypsin-EDTA was purchased from Biological Industries (USA). 2-(4-Iodophenyl)-3-(4-nitrophenyl)-5-(2,4-disulfo-phenyl)-2H-tetrazolium monosodium salt (WST-1) was purchased from Roche (Germany), and Hoechst 33342, and propidium iodide (PI) were purchased from Serva (Israel), while phosphate buffer solution (PBS) was purchased from Sigma-Aldrich (USA). The toxic effects of phosphazene derivatives (**7**, **8**, **9a**–**c**, and **10a**–**c**) on L929 fibroblasts and A549 lung cancer cells was determined using WST-1 assay, a colorimetric method for measuring cell cytotoxicity. L929 fibroblasts and A549 lung cancer cells were seeded into 96-well microassay plates at a density of 5×10^3 cells/well and cultured for 12 h. The compounds (**7**, **8**, **9a**–**c**, and **10a**–**c**) were sterilized by UV for 30 min before application, diluted with a cell culture medium (6.25, 12.5, 25, 50, and 100 µg/mL), inoculated into the wells, and incubated for 48

h. Only medium was exerted cells as a control. Next, the cell culture medium in each well was replaced with 100 µL of fresh medium and 15 µL of the WST-1 solution. After incubating for another 4 h at 37°C in dark at the incubator, the wells were read between 420-480 nm using an ELISA plate reader (BioTek, USA), and the percentage of viable cells was calculated. For WST-1 assay, the control L929 fibroblast and A549 lung cancer cell viability was defined as 100%. Only medium was replicated cells as a negative control. The samples were evaluated for each group, and different concentrations of each compound were examined as three repetitions.[38]

2.8. Determination of apoptosis and necrosis with double staining method

Apoptotic and necrotic effects of the phosphazene derivatives (**7**, **8**, **9a–c**, and **10a–c**) on L929 fibroblasts and A549 lung cancer cells were determined by double staining with Hoechst dye 3342 (2 µg/mL) and PI to quantify the number of apoptotic and necrotic cells. L929 fibroblast and A549 lung cancer cells ($2.5x10^4$ cells/well) were seeded into 24-well plates with DMEM solution. After being treated with different concentrations (6.25, 12.5, 25, 50, and 100 µg/mL) of the compounds (**7**, **8**, **9a–c**, and **10a–c**) for 48 h, attached and detached cells were harvested. Cells were washed with PBS and incubated with Hoechst dye 3342 (2 µg/mL), PI (1 µg/mL) and DNAse free-RNAse (100 µg/mL) for 15 min at room temperature. Next, 10-50 µL of cell suspension was smeared on a glass slide and coverslipped for examination under a fluorescence microscope (Leica DMI6000, Germany). In the double staining method with Hoechst dye and PI, the nuclei of normal cells are stained light blue whereas apoptotic cells are stained dark blue. The apoptotic cells were identified by their nuclear morphology based on nuclear fragmentation or chromatin condensation. Necrotic cells are stained red by PI. Since necrotic cells, lack of plasma membrane integrity, PI dye can cross the cell membrane unless it is intact. The number of apoptotic and necrotic cells in 10 random microscopic fields was counted, and the number of apoptotic and necrotic cells was determined with 4',6-diamidino-2-phenylindole (DAPI) and fluorescein isothiocyanate (FITC) filters of the fluorescence microscope. Data were expressed ratios of apoptotic or necrotic cells to normal cells. Different concentrations of each compound were examined as three repetitions.[39]

3. Results and discussion

3.1. Chemistry

The tentative reaction pathways suggested for the reactions of $N_3P_3Cl_6$ with tetradentate dibenzo-diaza podands (**3** and **4**) were given in Scheme 1. The possible reaction mechanisms SN^1 (P) and SN′ (P) (internal reaction) appear in the Scheme 1. The reactions of $N_3P_3Cl_6$ with equimolar amounts of dipotassium salts of dibenzo-diaza podands K_2(**3**) and K_2(**4**) produced **sbs** (**5** and **6**) and **sas** (**7** and **8**) cyclotriphosphazenes in THF. The formation of **sas** and **sbs** skeletons seems to proceed by SN^1 (P) and SN′ (P) involving the intermediate (**I**) (Scheme 1). Evidence for the formation of the 6-membered *spiro* ring of the intermediate (**I**) with the geminal substitution in the first step arises from the formation of a *bino* bridge for the **sbs** skeleton[30] with an *ansa* ring for the **sas** skeleton. Generally, triethylamine or excessive amine has been used to remove the liberated HCl as NEt_3.HCl or amine.HCl, respectively, in the nucleophilic substitution reactions of chlorocyclophosphazenes with amines. The reactions were performed using (i) and not using (ii) triethylamine. The 1:2 molar ratio reactions of $N_3P_3Cl_6$ and K_2(**3**) and K_2(**4**) in the absence of triethylamine induced greater yields of **sbs** (**5**, yield 47%; **6**, yield 25) and lower yields of **sas** (**7**, yield 35%; **8**, yield 18%) structures. The yields of **sas** products (**7** and **8**) were greater than those of **sbs** products (**5** and **6**) in the presence of triethylamine as an HCl acceptor and in a 1:1 molar ratio reaction of $N_3P_3Cl_6$ and K_2(**3**) and K_2(**4**), respectively. Such results may have been caused by the formation of intermolecular hydrogen bonding involving triethylamine and N–H hydrogen in the intermediate (**I**) (i, Scheme 1). In addition, the yields of both **sas** (**7** and **8**) and **sbs** (**5** and **6**) cyclotriphosphazenes also depended on the chain lengths R=$(CH_2)_n$ of dibenzo-diaza podands. For instance, the yields of **sas** (**7**, 65%) and **sbs** (**5**, 20%) products, which have the smallest alkyl chains R=$(CH_2)_3$, are greater than those of **sas** (**8**, 53%) and **sbs** (**6**, 17%) products with R=$(CH_2)_4$ alkyl chains. On the other hand, the formation of P–O bonds in *ansa* ring can take place in a *cis* fashion for the **sas** skeletons according to the crystallographic data of **sas 8** discussed in this paper's ''3.4. X-ray crystallography''. Hence, the *ansa-cis* products for the **sas** skeletons are isolated regioselectively from the replacement reactions of $N_3P_3Cl_6$ with dipotassium salts of tetradentate dibenzo-diaza podands. The reactions of partly substituted **sbs 7** and **8** phosphazenes with excess pyrrolidine, AEM and DASD in

THF produced fully substituted **sas** (**9a** and **10a**), (**9b** and **10b**), and (**9c** and **10c**) phosphazene derivatives, respectively.

In the literature, only *spiro* phosphazenes have been obtained from the reaction of $N_3P_3Cl_6$ with propane-1,3-diamine and butane-1,4-diamine.[40] Our research team recently prepared the first examples of *bino* (**5** and **6**) and *ansa* (**7** and **8**) structures with propane-1,3-diamine and butane-1,4-diamine precursors. Therefore, **sas** (**9b**, **9c** and **10a**–**c**) have become extended new compounds. Elemental analyses of the compounds are consistent with the structures, and fragments were observed under electrospray ionization mass spectrometry (ESI–MS) conditions. All substituted phosphazenes produced protonated molecular ions $[MH]^+$, which are the parent peaks in relative intensity. In the unimolecular decompositions of **sas** phosphazenes, the major fragmentation pathway involved the initial cleavage of the exocyclic P–N bond with the loss of heterocyclic amine groups.

3.2. FTIR spectroscopy

The FTIR spectra of substituted **sas** (**9b**, **9c** and **10a**–**c**) phosphazenes exhibited strong absorption frequencies in the range of 1211–1171 cm^{-1} ascribed to $\nu_{P=N}$ bands of the phosphazene ring. The aromatic C–H stretching bands were observed between 3045 and 3070 cm^{-1}. The most characteristic bands of the AEM and DASD substituted cyclotriphosphazenes were assigned to the C–O–C etheric bonds in the range of 1115–1155 cm^{-1}. Additionally, the IR spectra of AEM substituted phosphazenes displayed N–H stretching absorptions at approximatelly 3330 cm^{-1}. The partly substituted **sas** (**7** and **8**) gave stretching frequencies of PCl_2 bonds at 583 and 550 cm^{-1}, respectively. These bands disappear in the IR spectra of fully heterocyclic amine substituted phosphazenes.

3.3. NMR spectroscopy

The proton-decoupled ^{31}P NMR spectra of the fully substituted cyclotriphosphazenes (**9a**–**c** and **10a**–**c**) exhibited an A_2X spin system with two sets of peaks in a doublet-triplet pattern, assigned to the two OPN and one PX_2 phosphorus atoms (Table 3). The signals of δPX_2 of **9a**–**c** and **10a**–**c** shifted upfield by approximately 8.0 ppm with respect to the corresponding δPCl_2 of **7** and **8**, respectively, probably given the release of their lone electron pairs of the heterocyclic amine N–atoms to P–atoms.

The values of the two-bond coupling constants $^{2}J_{(P,P)}$ for fully substituted phosphazenes were far smaller than those of the partly substituted ones.

Table 3 ^{31}P NMR Data ($CDCl_3$) of **7**, **8**, **9a**–**c**, and **10a**–**c** (δ in ppm, J in Hz)

Compound	Spin system	δPCl_2	δPX_2	δOPN	$^{2}J_{PP}$
(**7**)[a]	A_2X	P_X:32.28	–	P_A:15.95	$^{2}J_{AX}$:69.4
(**8**)[a]	A_2X	P_X:32.28	–	P_A:15.83	$^{2}J_{AB}$:69.4
(**9a**)[b]	A_2X	–	P_X:22.20	P_A:19.50	$^{2}J_{AB}$:56.6
(**9b**)	A_2X	–	P_X:23.60	P_A:18.50	$^{2}J_{AB}$:59.3
(**9c**)	A_2X	–	P_X:25.90	P_A:19.00	$^{2}J_{AB}$:58.4
(**10a**)	A_2X	–	P_X:22.60	P_A:16.55	$^{2}J_{AB}$:54.0
(**10b**)	A_2X	–	P_X:23.00	P_A:15.90	$^{2}J_{AB}$:58.7
(**10c**)	A_2X	–	P_X:25.90	P_A:15.80	$^{2}J_{AB}$:55.8

[a] The values are taken from the literature.[30]

[b] The spectral data are available in the literature[30] and were re-recorded for comparison purposes.

^{1}H and ^{13}C NMR assignments of the compounds are summarized in Table 4. The assignments were made unambiguously by HSQC using values corresponding to $^{1}J_{(CH)}$ and by HMBC using values corresponding to $^{2}J_{(CH)}$, $^{3}J_{(CH)}$, $^{4}J_{(CH)}$, and $^{spatial}J_{(CH)}$ between the protons and carbons (Table 1S, S: designates supplementary info). HSQC spectra of **10a** (Fig. 1), **9b** (Fig. 1S), and **9c** (Fig. 2S) and HMBC spectra of **9b** (Fig. 3S) and **9c** (Fig. 4S) are given as examples.

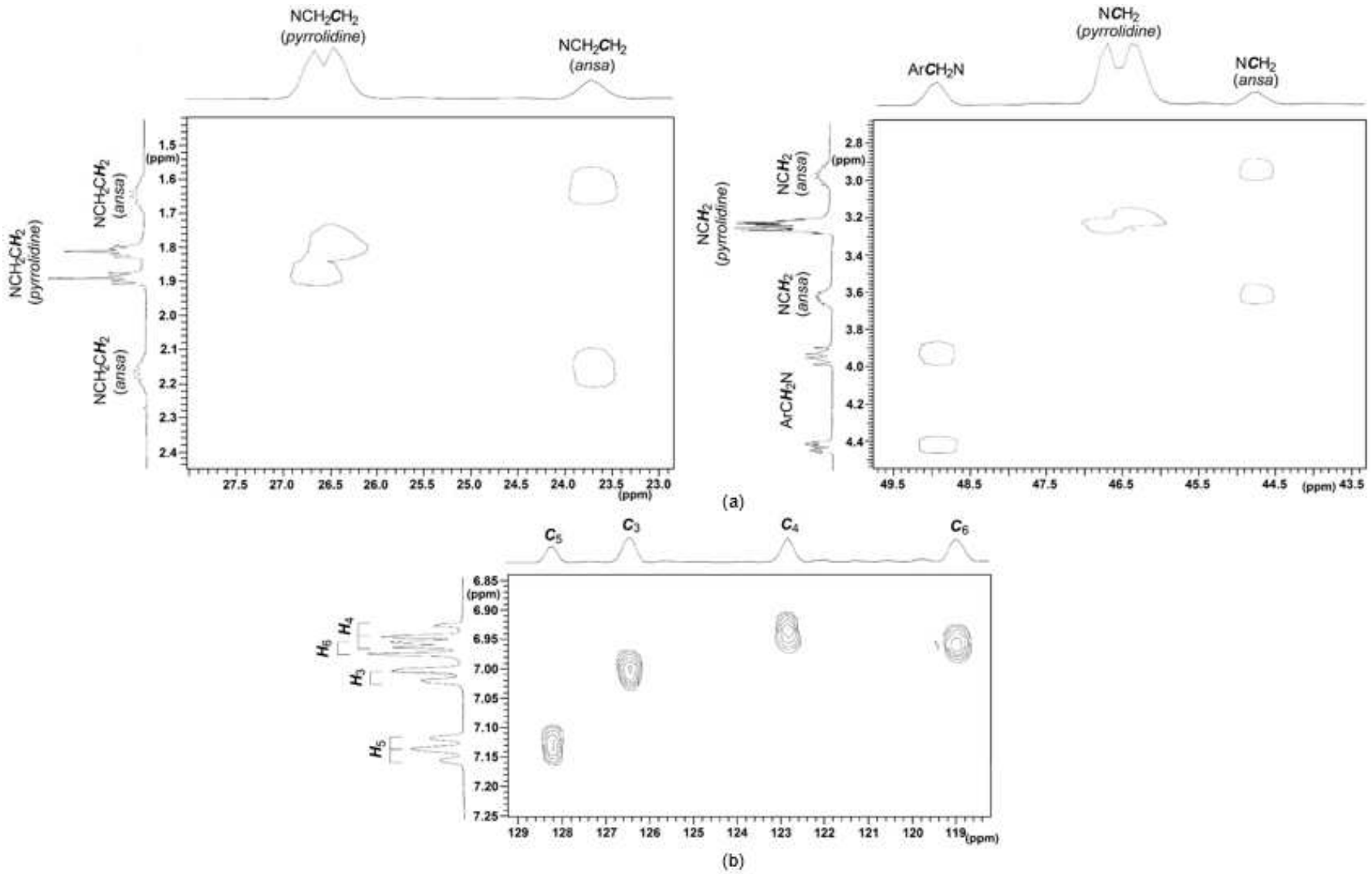

Fig. 1 HSQC spectrum (a) for the aliphatic and (b) aromatic regions of **10a**.

The aliphatic regions of the ^{1}H NMR spectra of the **sas** compounds are especially complex since all aliphatic protons are diastereotopic. The $NCH_2C\boldsymbol{H}_2$ and $NC\boldsymbol{H}_2$ proton signals of the heterocyclic amines were easily distinguished from those of the *ansa* rings by the HSQC spectra of **9a**–**c** and **10a**–**c**. In the ^{1}H NMR spectra of the substituted **sas** compounds, the substituent protons were observed as the pair of signals, indicating that the two geminal substituents are not equivalent (see a schematic representation of **sas** structure in Table 4). The $ArC\boldsymbol{H}_2$ benzylic protons of **sas** derivatives were separated from each other as two peak groups, indicating that the $ArC\boldsymbol{H}_2$ protons were not equivalent. As expected, the four different proton signals of the aromatic rings for the phosphazene derivatives were two sets of doublets and triplets.

All expected carbon peaks were assigned from the ^{13}C NMR spectra of the compounds. The most reliable evidence gathered from the substitution of all Cl–atoms of partly substituted **sas** (**7** and **8**) was the carbon signals of the substituents, which were observed in the ^{13}C NMR spectra. The $NCH_2\boldsymbol{C}H_2$ and $N\boldsymbol{C}H_2$ carbon signals of the *ansa* rings of **9a**–**c** and **10a**–**c** were distinguished from the corresponding carbon signals of the heterocyclic amine precursors. In the ^{13}C NMR spectra of the substituted derivatives, the geminal heterocyclic amine substituents showed two groups of $NCH_2\boldsymbol{C}H_2$ (except **9a**) and $N\boldsymbol{C}H_2$ signals with small separations. The results also indicate that the two geminal groups were not equivalent to each other. The same situation was also observed for $O\boldsymbol{C}H_2$ (except **9b**) and $O\boldsymbol{C}O$ carbons. For all **sas** phosphazenes, the couplings $^{2}J_{PC1}$, $^{3}J_{PC2}$, and $^{3}J_{PC6}$ were observed as triplets, indicating the second-order effects previously observed.[41] The J_{PC} coupling constants between the external transitions of the triplets were estimated.

Table 4 ^{1}H and ^{13}C NMR Data ($CDCl_3$) of **9a–c** and **10a–c** (δ in ppm, J in Hz, s: *singlet*, d: *doublet*, t: *triplet*, and m: *multiplet* peak)

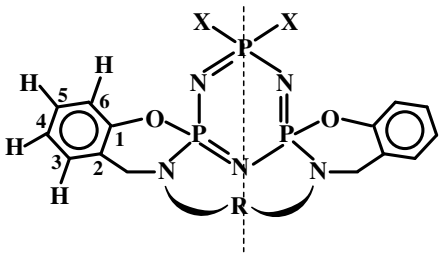

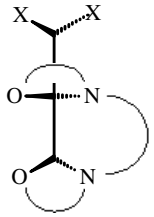

Schemetic representative structure of **sas**

	(**9a**)[a]	(**9b**)	(**9c**)	(**10a**)	(**10b**)	(**10c**)
H						
NCH_2CH_2	*ansa* 1.62 (m,1H) 2.04 (m,1H) *pyrrolidine* 1.83 (m,4H) 1.87 (m,4H)	*ansa* 1.61 (m,1H) 2.09 (m,1H) *AEM* 2.50 (m,4H)	*ansa* 1.62 (m,1H) 2.04 (m,1H) *DASD* 1.68 (t,4H) $^3J_{HH}$=5.6 1.78 (t,4H) $^3J_{HH}$=5.6	*ansa* 1.62 (m,2H) 2.16 (m,2H) *pyrrolidine* 1.80 (m,4H) 1.88 (m,4H)	*ansa* 1.26 (m,2H) 1.68 (m,2H) *AEM* 2.46 (m,4H)	*ansa* 1.64 (m,2H) 2.04 (m,2H) *DASD* 1.68 (t,4H) $^3J_{HH}$=5.3 1.85 (t,4H) $^3J_{HH}$=5.3
NCH_2	*ansa* 3.32 (m,2H) 3.48 (m,2H) *pyrrolidine* 3.25 (m,4H) 3.28 (m,4H)	*ansa* 3.34 (m,2H) 3.45 (m,2H) *AEM* 2.53 (m,2H) $^3J_{HH}$=5.2 2.58 (m,2H) $^3J_{HH}$=5.8 $^2J_{HH}$=20.4 *AEM (morph.)* 3.12 (m,4H) $^3J_{HH}$=5.2 3.14 (m,4H) $^3J_{HH}$=5.4	*ansa* 3.24-3.44 (m,4H) *DASD* 3.24-3.44 (m,8H)	*ansa* 2.95 (m,2H) 3.62 (m,2H) *pyrrolidine* 3.21 (m,4H) 3.24 (m,4H)	*ansa* 3.23 (m,2H) 3.34 (m,2H) *AEM* 2.49 (m,2H) $^3J_{HH}$=4.8 2.54 (m,2H) $^3J_{HH}$=5.6 $^2J_{HH}$=18.8 *AEM (morph.)* 3.02 (m,4H) $^3J_{HH}$=5.2 3.06 (m,4H) $^3J_{HH}$=6.0	*ansa* 3.3 (m,4H) *DASD* 2.96 (m,4H) 3.95 (m,4H)
OCH_2	—	3.69 (t,4H) $^3J_{HH}$=4.4 3.74 (t,4H) $^3J_{HH}$=4.4	3.95 (s,4H) 3.96 (s,4H)	—	3.67 (t,4H) $^3J_{HH}$=4.2 3.71 (t,4H) $^3J_{HH}$=4.2	3.95 (s,4H) 4.00 (s,4H)
$ArCH_2N$	3.84 (m,2H) 4.48 (m,2H)	4.07 (m,2H) 4.32 (m,2H)	4.10 (m,2H) 4.24 (m,2H)	3.93 (m,2H) 4.42 (m,2H)	4.18 (m,2H) 4.26 (m,2H)	4.40 (m,2H) 4.43 (m,2H)
Ar***H*** H_3	6.99 (d,2H)	7.02 (d,2H)	6.98 (d,2H)	6.99 (d,2H)	7.01 (d,2H)	7.01 (d,2H)
H_4	6.94 (t,2H)	6.96 (t,2H)	6.93 (t,2H)	6.93 (t,2H)	7.00 (t,2H)	6.95 (t,2H)
H_5	7.13 (t,2H)	7.15 (t,2H)	7.12 (t,2H)	7.12 (t,2H)	7.20 (t,2H)	7.15 (t,2H)
H_6	6.96 (d,2H)	6.95 (d,2H)	6.96 (d,2H)	6.94 (d,2H)	6.94 (d,2H)	6.98 (d,2H)
$^3J_{3-4}$	6.0	6.8	7.2	7.2	8.8	8.0
$^3J_{4-5}$	7.7	7.4	7.7	7.8	8.0	7.6
$^3J_{5-6}$	7.2	7.6	9.2	8.4	8.0	7.2

C							
$NCH_2\boldsymbol{C}H_2$		*ansa* 25.4 *pyrrolidine* 26.6 $^3J_{PC}$=9.2	*ansa* 25.1 *AEM* 53.5 53.7	*ansa* 23.5 *DASD* 35.6 $^3J_{PC}$=6.1 35.9 $^3J_{PC}$=6.1	*ansa* 23.7 *pyrrolidine* 26.4 $^3J_{PC}$=10.0 26.5 $^3J_{PC}$=9.3	*ansa* 25.4 *AEM* 53.5	*ansa* 23.4 *DASD* 35.3 $^3J_{PC}$=6.8 35.7 $^3J_{PC}$=7.5
$N\boldsymbol{C}H_2$		*ansa* 48.9 *pyrrolidine* 46.4 $^2J_{PC}$=4.6 46.6 $^2J_{PC}$=3.8	*ansa* 49.2 *AEM* 59.2 $^3J_{PC}$=7.7 59.3 $^3J_{PC}$=7.6 *AEM (morph.)* 37.0 37.8	*ansa* 48.9 *DASD* 42.7 $^2J_{PC}$=3.1 43.1 $^2J_{PC}$=3.1	*ansa* 44.7 *pyrrolidine* 46.3 $^2J_{PC}$=3.8 46.7 $^2J_{PC}$=3.8	*ansa* 47.6 *AEM* 59.0 $^3J_{PC}$=7.6 59.1 $^3J_{PC}$=7.6 *AEM (morph.)* 37.2 37.3	*ansa* 44.4 *DASD* 42.4 $^2J_{PC}$=2.3 43.0 $^2J_{PC}$=3.9
$O\boldsymbol{C}H_2$		—	67.2	64.4 64.5	—	67.1 67.2	64.3 64.2
$O\boldsymbol{C}O$		—	—	107.2 107.9 $^4J_{PC}$=1.5	—	—	107.5 107.9
$Ar\boldsymbol{C}H_2N$		49.5	49.5	49.5	48.9	48.4	48.7
$Ar\boldsymbol{C}$	$\boldsymbol{C}_1$	151.6 $^2J_{PC}$=6.8	151.2 $^2J_{PC}$=6.1	151.4 $^2J_{PC}$=6.1	151.4 $^2J_{PC}$=7.6	150.8 $^2J_{PC}$=7.4	151.0 $^2J_{PC}$=7.6
	$\boldsymbol{C}_2$	123.6 $^3J_{PC}$=7.7	123.5 $^3J_{PC}$=7.6	123.5 $^3J_{PC}$=7.7	124.6 $^3J_{PC}$=6.1	124.0 $^3J_{PC}$=7.6	124.0 $^3J_{PC}$=6.1
	$\boldsymbol{C}_3$	126.7	126.7	126.6	126.3	126.9	126.2
	$\boldsymbol{C}_4$	122.8	123.1	123.0	122.8	123.7	122.7
	$\boldsymbol{C}_5$	128.3	128.5	128.4	128.2	128.8	128.1
	$\boldsymbol{C}_6$	119.2 $^3J_{PC}$=9.3	119.0 $^3J_{PC}$=9.2	119.2 $^3J_{PC}$=9.3	119.0 $^3J_{PC}$=9.3	118.7 $^3J_{PC}$=8.5	118.8 $^3J_{PC}$=8.5

[a] The spectral data are available in the literature[30] and were re-recorded for comparison purposes.

3.4. X-ray crystallography

The molecular and solid state structure of **8** with the atom-numbering scheme is depicted in Fig. 2. The asymmetric unit of **8** contained one uncoordinated benzene molecule. As shown in the packing diagram of **8** (Fig. 5S), the benzene molecules filled the cavities between the cyclotriphosphazene molecules. The intermolecular C–H…O^{i} hydrogen bond [C16–H16 (0.930 Å); H16…O1^{i} (2.608(3) Å); C16…O1^{i} (3.464(6) Å); C16–H16…O1^{i} (153.24(0.29)^{o}); symmetry code: (i) –x+1, –y, –z+1] dimerized two phosphazene molecules, and dipole-dipole and van der Waals interactions were effective in molecular packing. There was also an intramolecular C–H…N hydrogen bond [C9–H9B (0.970(6) Å); H9B…N2 (2.571(3) Å); C9…N2 (3.221(7) Å); C9–H9B…N2 (124.43(0.37)^{o})]. The phosphazene ring had a pseudo-mirror plane according to the torsion angles (Fig. 6S) and was in twisted conformation [Fig. 7Sa; φ_2 = –176.2(1)°, θ_2 = 66.1(1)° (P1/N1/P2/N2/P3/N3)] with total puckering amplitude[42] Q_T of 0.205(2) Å. The nine-membered *ansa* ring (P2/N2/P3/N4/C8/C9/C10/C11/N5) and six-membered *spiro* rings (P2/N5/C12/C13/C18/O2) and (P3/O1/C1/C6/C7/N4) were also in twisted conformations (Fig. 7Sb), Fig. 7Sc: Q_T = 1.180(5) Å, φ_2 = –116.2(5)°, φ_3 = –70.3(3)°, φ_4 = –127.0(8)°, θ_2 = 36.0(3)°, θ_3 = 69.9(3)° (P2/N2/P3/N4/C8/C9/C10/C11/N5); Fig. 7Sd: Q_T = 0.540(4) Å, φ_2 = –71.4(7)°, θ_2 = 141.3(4)° (P2/N5/C12/C13/C18/O2); Fig. 7Se: Q_T = 1.122(5) Å, φ_2 = –77.5(3)°, θ_2 = 133.6(3)° (P3/O1/C1/C6/C7/N4). By contrast, the bicyclic system made of phosphazene and *ansa* rings of **8** was in a sofa conformation (Fig. 7Sf) and contained V-shaped rings with two nonplanar halves (P2/N1/P1/N3/P3) and (P3/N4/C8/C9/C10/C11/N5/P2), one of which (P2/N1/P1/N3/P3) was essentially planar, while the other (P2/N5/C9/C8/N4/P3) was in a crown conformation (Fig. 7Sg). The atoms P2 and P3 each had four different attachments, and P2–O2 and P3–O1 were bonded in *cis* fashion. Hence, both might represent stereogenic centers given their (*R*)- and (*S*)-configurations (*meso* form). The analogous **sas** cyclotriphosphazenes (**7**, **9a**–**c**, and **10a**–**c**) were likely to have (*R*)- and (*S*)-configurations (*meso* form). In the literature, the PN single and double bonds are generally in the ranges of 1.628–1.691 Å and 1.571–1.604 Å, respectively.[43] The endocyclic PN bond lengths of **8** (1.560(3)–1.605(3) Å; see Table 3) were in agreement with these findings. Eventually, the double-bond character and variation of endo- and exocyclic bond angles of phosphazene ring for **8** could be explained by the negative hyperconjugation model.[44] The average endocyclic PN bond lengths of **8** was 1.581(3) Å which is considerably shorter than the average exocyclic PN bonds [1.636(3) Å]. In the phosphazene ring, the

endocyclic angles N2–P3–N3 and N1–P2–N2 [113.6(2)° and 114.6(2)°] decreased regarding the corresponding value in the ''standard'' compound $N_3P_3Cl_6$ [118.3(2)°].[45] The P2–N2–P3 and C8–C9–C10 bond angles were quite large due to the crown conformation of the nine-membered *ansa* ring. The corresponding PNP angles of the analogous compounds [114.1° for R=$(CH_2)_2$ and X=Cl,[46] 122.6° for R=$(CH_2)_2$ and X=morpholine,[47] and 113.2° for R=$(CH_2)_2$ and X=DASD[29]] varied according to *ansa* chain length [R=$(CH_2)_n$] and substituent type (Cl and/or heterocyclic amines).

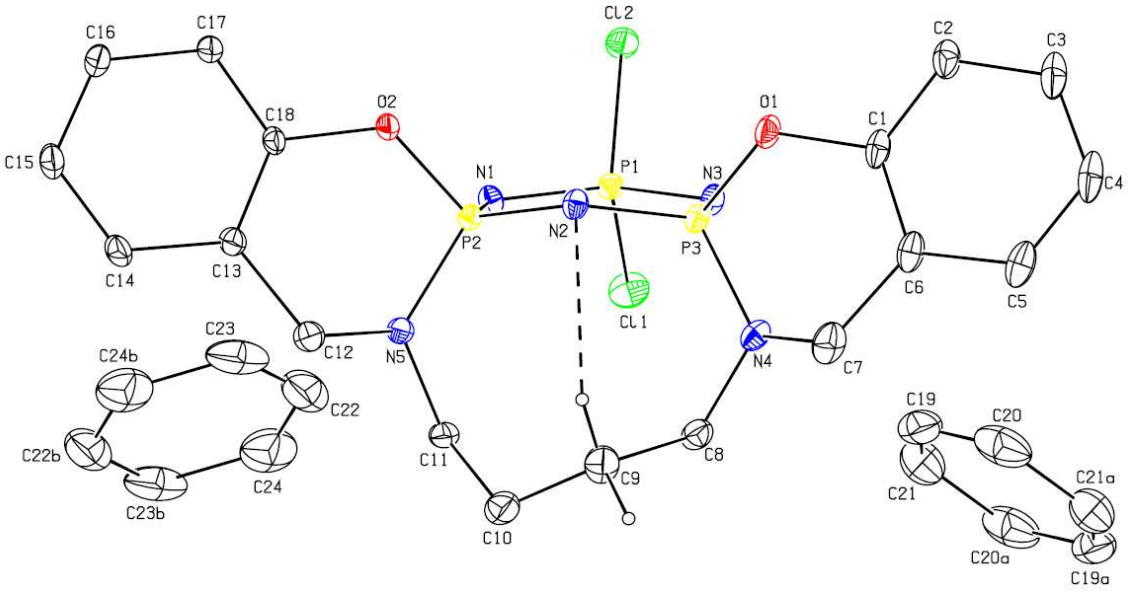

Fig. 2 ORTEP-3 drawing of **8** with the atom-numbering scheme. Displacement ellipsoids are drawn at a 30% probability level.

3.5. Antimicrobial activity

The starting compound ($N_3P_3Cl_6$), pyrrolidine, AEM, DASD and dibenzo-diaza podands (**3** and **4**) were subjected to antimicrobial activity against the bacteria and yeast strain tested for phosphazene derivatives (**5**–**8**, **9a**–**c**, and **10a**–**c**) for comparison in this study. Antimicrobial activity, minimum inhibitory concentrations (MIC), minimal bactericidal concentrations (MBC), and minimal fungicidal concentrations (MFC) of $N_3P_3Cl_6$, pyrrolidine, AEM, DASD, dibenzo-diaza podands (**3** and **4**), and phosphazene derivatives are given in Tables 5-7, respectively. The concentrations of the compounds were 5000 µM in 1,4-dioxane, which had no effect on the pathogenic bacteria and fungus at any

concentration. The starting compounds $N_3P_3Cl_6$, heterocyclic amines and dibenzo-diaza podands (**3** and **4**)] and phosphazene derivatives (**6**, **8**, **10a**, and **10b**) possessed antibacterial activity against *E.coli* 35218. Phosphazene **7** was very active against *S. aureus*, *B. subtilis*, *E. faecalis, E. coli* 25922, according to MIC values. The MICs of the compounds were studied further; their values range from 78 µM to >1250 µM (Table 6).

In the literature, some phenoxyphosphazenes with oxime and/or Schiff base groups were effective against *E. coli* and *S. aureus*.[48,49] Our team observed that pyrolidine substituted phosphazenes bearing N/O-,[50] 4-fluoro-benzyl-[36] and ferrocenyl-[13,51–53] *spiro*cyclic groupswere active against *E. coli*, *S. aureus*, *B. cereus* and *B. subtilis* bacteria, as well as *C. albicans* and *C. tropicalis* fungi. In addition, the fully pyrrolidinyl-substituted **sbs** phosphazene [$R=(CH_2)_2$] was found to be moderately effective against *C. tropicalis*.[47] The basic requirement for antimicrobial activity of cyclotriphosphazene derivatives in this study were likely to be chain length of the alkane diamine precursor [$R=(CH_2)_n$, n=2,3,4] and substituents (Cl or heterocyclic amine groups) bonded to P–atoms, the phosphazene skeleton, and/or the compound itself. Considering the alkane diamine precursors for **sbs 6** [$R=(CH_2)_4$] and **5** [$R=(CH_2)_3$] and the analogous compound $R=(CH_2)_2$[47] that is, three compounds differing only by chain length of the *bino*-skeleton, the last two compounds exhibited no antibacterial activity against *E. coli* 35218. Based on the results of such antibacterial activity against *E. coli* 35218 of **sas 7** and **8** and the analogous [$R=(CH_2)_2$[47]] phosphazenes, the eight-membered *ansa* ring of **7** seems to be effective compared with the nine- and seven-membered *ansa* rings. In the case of heterocyclic amine-substituted **sas 9a**–**c**, **10a**–**c**, and the analogous phosphazene [$R=(CH_2)_2$, X=pyrrolidine[47]], the compounds **10a** and **10b**, which contained a nine-membered *ansa* ring, and pyrrolidine and AEM groups, respectively, were active against *E.coli* 35218. In addition, compounds **10a**–**c** displayed activity (9.0 ± 0.0) against yeast strain *C. albicans* compared with that of *Ketoconazole* (11.0 ± 1.0) (Table 5). Remarkably, the activities of **10a**–**c** may be attributed to the presence of the nine-membered *ansa* ring instead of to heterocyclic amine type, suggesting that the antimicrobial activity of the phosphazene derivatives varies depending on whether the substituents bonded to the P–atoms, phosphazene skeleton, and/or the compound itself.

Table 5 The antimicrobial activity of $N_3P_3Cl_6$, pyrrolidine, AEM, DASD, dibenzo-diaza podands (**3** and **4**), 1,4-dioxane, and cyclotriphosphazene derivatives (**5**–**8**, **9a**–**c**, and **10a**–**c**) expressed as inhibition zones (mm) at 5000 µM (Antibiotics; Amp= *Ampicillin*, C= *Chloramphenicol* and Keto= *Ketoconazole*)

	Test Bacteria and yeast strain							
	S. aureus **ATCC 25923**	***B. subtilis*** **ATCC 6633**	***B. cereus*** **NRRL-B-3711**	***E. faecalis*** **ATCC 292112**	***P. aeruginosa*** **ATCC 27853**	***E. coli*** **ATCC 25922**	***E. coli*** **ATCC 35218**	***C. albicans*** **ATCC 10231**
Amp	44.0 ± 1.0	23.0 ± 1.0	–	27.0 ± 0.0	60.0 ± 0.0	18.0 ± 0.0	–	–
C	24.0 ± 1.0	21.0 ± 0.0	–	20.0 ± 0.0	34.0 ± 0.0	25.0 ± 0.0	8.0 ± 0.0	–
Keto	–	–	–	–	–	–	–	11.0 ± 1.0
$N_3P_3Cl_6$	9.0 ± 0.0	10.0 ± 0.0	10.0 ± 0.0	11.0 ± 0.0	11.0 ± 0.0	13.0 ± 1.0	12.0 ± 1.0	9.0 ± 0.0
pyrrolidine	–	–	–	–	–	10.0 ± 1.0	9.0 ± 0.0	9.0 ± 0.0
AEM	–	–	–	–	–	11.0 ± 0.0	10.0 ± 0.0	10.0 ± 0.0
DASD	–	–	–	9.0 ± 0.0	10.0 ± 1.0	11.0 ± 1.0	10.0 ± 0.0	9.0 ± 0.0
1,4-Dioxane	–	–	–	–	–	–	–	–
(**3**)	–	–	10.0 ± 0.0	10.0 ± 0.0	10.0 ± 1.0	10.0 ± 0.0	11.0 ± 0.0	10.0 ± 0.0
(**4**)	–	–	11.0 ± 0.0	–	–	10.0 ± 0.0	11.0 ± 0.0	9.0 ± 0.0
(**5**)	–	–	–	–	–	–	–	–
(**6**)	–	–	–	–	10.0 ± 0.0	–	12.0 ± 0.0	–
(**7**)	20.3 ± 0.6	17.7 ± 0.6	15.0 ± 1.7	18.7 ± 1.5	–	18.3 ± 2.9	–	–
(**8**)	–	–	11.0 ± 1.7	–	–	–	10.3 ± 0.6	–
(**9a**)	–	–	–	–	–	–	–	–
(**9b**)	–	–	–	–	8.3 ± 1.5	–	–	–
(**9c**)	–	–	9.0 ± 1.7	–	9.7 ± 0.6	–	–	–
(**10a**)	11.0 ± 1.0	–	11.0 ± 1.0	–	10.0 ± 1.0	12.0 ± 0.0	12.0 ± 0.0	9.0 ± 0.0
(**10b**)	–	9.0 ± 0.0	–	–	10.0 ± 0.0	12.0 ± 1.0	9.0 ± 1.0	9.0 ± 0.0
(**10c**)	–	–	–	–	10.0 ± 1.0	12.0 ± 0.0	–	9.0 ± 0.0

Values represent averages for triplicate experiments, and the deviation values are 0.0 when three measurements exactly the same.

Table 6 The antimicrobial activity of $N_3P_3Cl_6$, pyrrolidine, AEM, DASD, dibenzo-diaza podands (**3** and **4**), and cyclotriphosphazene derivatives (**6**–**8** and **10a**–**c**) as minimum inhibitory concentration (MIC) values (μm)

	Test Bacteria and yeast strain							
	S. aureus **ATCC 25923**	***B. subtilis*** **ATCC 6633**	***B. cereus*** **NRRL-B-3711**	***E. faecalis*** **ATCC 292112**	***P. aeruginosa*** **ATCC 27853**	***E. coli*** **ATCC 25922**	***E. coli*** **ATCC 35218**	***C. albicans*** **ATCC 10231**
$N_3P_3Cl_6$	78	78	78	156	39	78	156	39
Pyrrolidine	–	–	–	–	–	78	312.5	78
AEM	–	–	–	–	–	156	156	78
DASD	–	–	–	156	78	156	156	78
(**3**)	–	–	78	156	78	156	156	78
(**4**)	–	–	78	–	–	78	156	78
(**6**)	–	–	–	–	78	–	312.5	–
(**7**)	625	156	625	156	–	156	–	–
(**8**)	–	–	>1250	–	–	–	312.5	–
(**10a**)	625	–	78	–	78	78	312.5	78
(**10b**)	–	156	–	–	78	78	312.5	78
(**10c**)	–	–	–	–	78	156	–	78

Table 7 Minimal bactericidal concentrations (MBC) and minimal fungicidal concentrations (MFC) of $N_3P_3Cl_6$, pyrrolidine, AEM, DASD, dibenzo-diaza podands (**3** and **4**), and cyclotriphosphazene derivatives (**6**–**8** and **10a**–**c**) (μm)

	Test Bacteria and yeast strain							
	MBC							MFC
	S. aureus **ATCC 25923**	***B. subtilis*** **ATCC 6633**	***B. cereus*** **NRRL-B-3711**	***E. faecalis*** **ATCC 292112**	***P. aeruginosa*** **ATCC 27853**	***E. coli*** **ATCC 25922**	***E. coli*** **ATCC 35218**	***C. albicans*** **ATCC 10231**
$N_3P_3Cl_6$	156	78	78	156	39	312.5	312.5	39
Pyrrolidine	–	–	–	–	–	312.5	312.5	78
AEM	–	–	–	–	–	156	312.5	78
DASD	–	–	–	312.5	78	156	312.5	78
(**3**)	–	–	78	156	78	156	156	78
(**4**)	–	–	156	–	–	78	156	78
(**6**)	–	–	–	–	156	–	312.5	–
(**7**)	625	156	>1250	156	–	312.5	–	–
(**8**)	–	–	>1250	–	–	–	312.5	–
(**10a**)	625	–	78	–	78	156	312.5	78
(**10b**)	–	156	–	–	156	78	312.5	78
(**10c**)	–	–	–	–	156	312.5	–	78

3.6. Interactions of DNA with the compounds

When circular plasmid DNA is subjected to electrophoresis, relatively fast mobility is observed in the intact supercoiled form I DNA. If a cleavage occurs on one strand (i.e., nicking), then the supercoil migrates more slowly as it relaxes to the open circular form II. When both DNA strands are cleaved, linear form III arises between forms I and II.[27] Fig. 3 gives the electrophoretograms applied to produce incubated mixtures of pBR322 DNA at varying concentrations (2500 to 312 µM) of the compounds. The results reveal that pyrrolidine, AEM, and **sbs 6** had no effect on plasmid DNA and that DASD only increased the mobility of form I DNA. However, $N_3P_3Cl_6$ converted the faster moving form I into a slower moving form II by nicking single and double strands of plasmid DNA. Therefore, we can conclude that $N_3P_3Cl_6$ causes significant conformational change. Meanwhile, phosphazene derivatives (**5**, **7**, **8**, **9b**, and **9c**) slightly increased the mobility of form I DNA, thereby indicating the degradative effect of phosphazene. In the case of **9a**, compound caused retardation on gel compared to the untreated plasmid DNA. The intensity of form I DNA was found to decrease substantially in the presence of **10a** and **10b**, though **10c** did not affect the intensity or mobility of the plasmid DNA.

3.7. Cytotoxicity screening of the compounds

The toxic effect of the cyclotriphosphazenes (**7**, **8**, **9a**–**c**, and **10a**–**c**) on L929 fibroblast and A549 lung cancer cells are illustrated in Figs. 4 and 5, respectively. Compounds at different concentrations within the range of 6.25-100 µg/mL were applied to the cells. Only medium was applied to the control group; the viability ratio in the group was accepted as 100%. According to the results obtained, while only **9a** showed a toxic effect at the rate of 16% at 100 µg/mL concentration in the fibroblast cells, no toxic effect was observed at different concentrations of other compounds (Fig. 4). When the compounds were applied to the A549 lung cancer cells, toxicity increased depending on the concentration. The highest toxic effect was obtained for **9c** at 100 µg/mL with a rate of 42%, and AEM and DASD substituted derivatives (**10b** and **10c**) were obtained at the rates of 32 and 30%, respectively, at the same concentration. It was observed that partly substituted phosphazene derivatives (**7** and **8**) showed the toxic effect at the rate of 24 and 28%, respectively, also at this concentration (Fig. 5). As a result, it

was determined that the toxicity of compounds against A549 lung cancer cells was greater than that against L929 fibroblast cells.

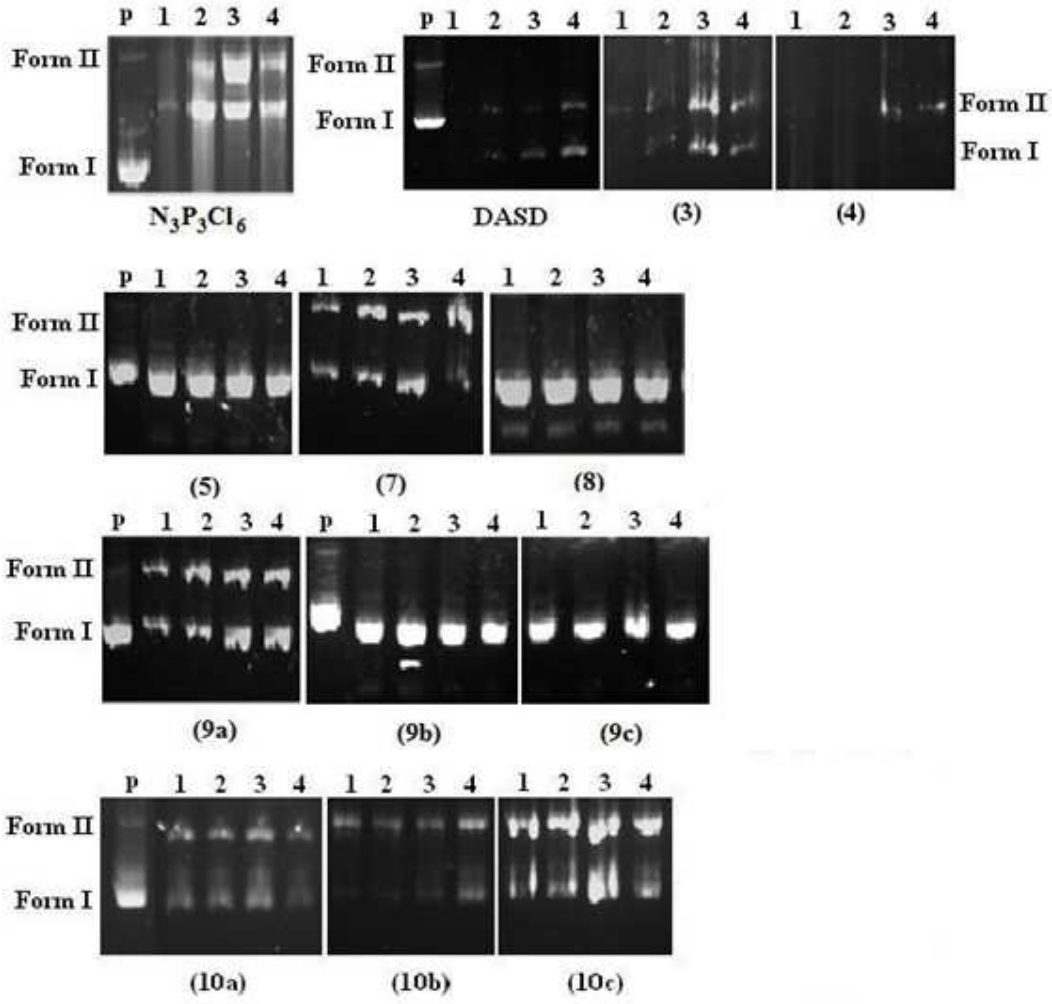

Fig. 3 Electrophoretograms of the interaction of pBR322 plasmid DNA with decreasing concentrations of $N_3P_3Cl_6$, DASD, **3**–**5**, **7**, **8**, **9a**–**c**, and **10a**–**c**. Untreated pBR322 plasmid DNA was applied to lane P. Concentrations (in μM) are as follows: lanes 1–4 apply to plasmid DNA interacting with decreasing concentrations of the compounds (lane 1: 2500; lane 2: 1250; lane 3: 625; lane 4: 312). The top and the bottom bands correspond to form II (single nicked open circular) and I (covalently closed circular or supercoiled) plasmids, respectively.

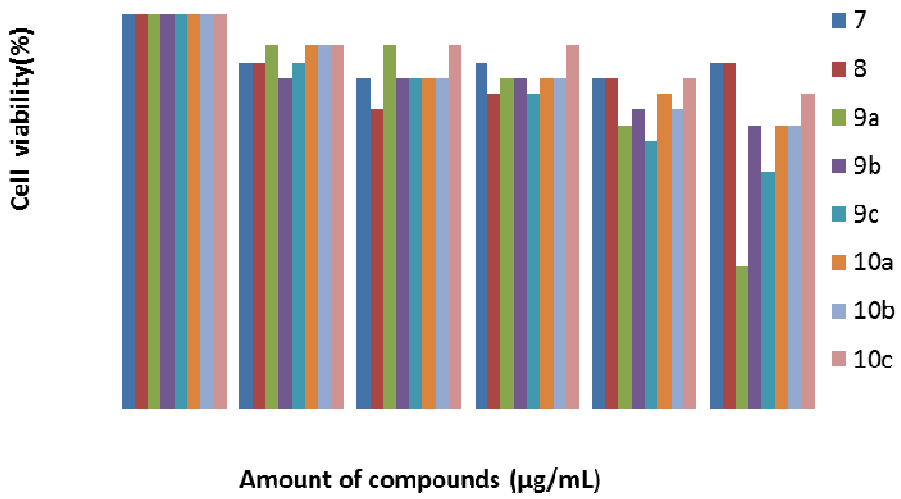

Fig. 4 The cytotoxic effect of compounds (**7**, **8**, **9a**–**c**, and **10a**–**c**) on L929 fibroblast cell line *in vitro*.

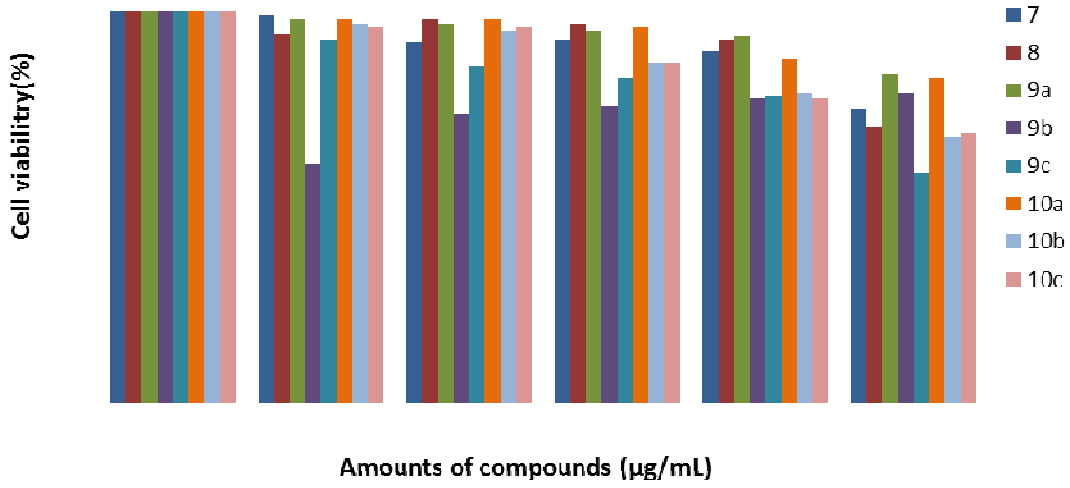

Fig. 5 The cytotoxic effect of compounds (**7**, **8**, **9a**–**c**, and **10a**–**c**) on A549 lung cancer cell line *in vitro*.

3.8. Apoptosis and necrosis

The apoptotic and necrotic effects of phosphazene derivatives (**7**, **8**, **9a**–**c**, and **10a**–**c**) on L929 fibroblast and A549 lung cancer cells are illustrated in Tables 8 and 9, respectively. When compounds were applied to L929 fibroblast cells at different concentrations, it was observed that the apoptotic effect increased depending on the concentration. Especially, **10a** at 100 µg/mL concentration caused the highest apoptosis at a rate of 34.2 ± 3% in L929 fibroblast cells. When compounds were applied to A549 lung cancer cells, even though the apoptotic effect changed with the concentration, no apoptotic effect at high rates was observed, and the rates were similar. The highest apoptotic effect in A549 lung cancer cell lines was obtained from **9b** at the rate of 21.6±2% (Table 9). Eventually, the apoptotic effect of the compounds was greater in L929 fibroblast cells than in A549 lung cancer cells.

When the necrotic effect of the phosphazene derivatives was examined, this situation differed from that of the apoptotic effect. When compounds were applied to L929 fibroblast cells at different rates, no concentration-dependent increase was observed. It was only noted that **9a** caused necrosis at 100 µg/mL concentration with the highest rate of 15 ± 2%. The results were found to be compatible with cytotoxicity results. When compounds were applied to A549 lung cancer cells, it was observed that necrotic effect increased depending on concentration (Table 9). The highest necrotic effect was obtained from **10b** at 33.7 ± 3% 100µg/mL concentration, while the necrotic effects of **7** and **9b** in the same concentration were found to be 26.2 ± 2 and 27.8 ± 2%, respectively. Consequently, the necrotic effects of compounds were greater in A549 lung cancer cells than in L929 fibroblast cells.

Table 8 Apoptotic and necrotic effects of cyclotriphosphazenes (**7**, **8**, **9a**–**c**, and **10a**–**c**) on L929 fibroblast cells line *in vitro*; data given with ± *SD*

Amount of compound µg/mL	Apoptotic ratio (%)								Necrotic ratio (%)							
	(**7**)	(**8**)	(**9a**)	(**9b**)	(**9c**)	(**10a**)	(**10b**)	(**10c**)	(**7**)	(**8**)	(**9a**)	(**9b**)	(**9c**)	(**10a**)	(**10b**)	(**10c**)
0	2±1	2±1	2±1	2±1	2±1	2±1	2±1	2±1	2±1	2±1	2±1	2±1	2±1	2±1	2±1	2±1
6.25	6.4±1	3.2±1	5.6±1	7.6±1	10.8±1	5.7±1	7.3±1	5.6±1	1.5±1	2±1	2±1	2±1	2±1	1±1	2±1	1±1
12.5	9.8±1	5.8±2	16.5±1	12.4±1	17.6±2	8.4±1	11.6±1	7.2±1	1±1	3±1	2±1	2±1	4±1	2±1	2±1	1±1
25	13.6±1	11.3±1	12.2±1	17.4±1	24.7±2	11.9±1	14.8±1	10.6±1	1±1	4±1	3±1	2±1	4±1	2±1	2±1	1±1
50	22.1±2	17.1±1	23.6±1	18.3±2	26.3±2	18.5±2	16.8±2	12.3±1	3±1	4±1	5±2	3±1	6±1	3±1	4±1	1±1
100	25.2±2	23.4±1	33.9±1	19.8±2	31.6±2	34.2±3	21.7±2	16.9±2	5±2	6±1	15±2	5±1	9±2	3±1	6±1	4±1

Table 9 Apoptotic and necrotic effects of cyclotriphosphazenes (**7**, **8**, **9a**–**c**, and **10a**–**c**) on A549 lung cancer cells line *in vitro*; data given with ± *SD*

Amount of compound µg/mL	Apoptotic ratio (%)								Necrotic ratio (%)							
	(**7**)	(**8**)	(**9a**)	(**9b**)	(**9c**)	(**10a**)	(**10b**)	(**10c**)	(**7**)	(**8**)	(**9a**)	(**9b**)	(**9c**)	(**10a**)	(**10b**)	(**10c**)
0	3±1	3±1	3±1	3±1	3±1	3±1	3±1	3±1	2±1	2±1	2±1	2±1	2±1	2±1	2±1	2±1
6.25	5.2±1	11.2±2	3.7±1	5.8±1	6.3±1	4.8±1	3±1	3±1	7.3±1	6.5±1	4.3±1	9.6±1	6.2±1	4.4±1	8.7±1	4.8±1
12.5	8.1±1	14.6±2	4.9±1	9.6±1	8.4±1	6.2±1	4.3±1	5.4±1	8.7±1	7.5±1	5.7±1	13.8±2	8.4±1	6.5±1	16.4±1	10.3±1
25	9.6±1	11.5±1	8.8±1	13.8±1	11.6±1	10.8±1	7.6±1	6.4±1	11.2±1	9.3±1	8.6±1	19.4±1	11.3±1	10.6±1	20.6±1	12.5±1
50	12.6±2	11.4±1	7.4±1	17.8±2	14.6±1	12.4±1	9.7±1	7.9±1	11.5±1	7.9±1	19.4±2	22.3±2	14.5±1	12.8±1	28.9±1	14.7±1
100	14.1±1	12.2±1	11.7±1	21.6±2	17.9±2	14.5±2	16.2±2	8.7±1	26.2±2	11.2±1	22.1±2	27.8±2	17.3±2	14.4±1	33.7±3	20.7±2

4. Conclusions

The fully substituted *spiro-ansa-spiro*-cyclotriphosphazenes (**9a**–**c** and **10a**–**c**) in this study were synthesized by means of Cl replacement reactions of partly substituted *spiro-ansa-spiro*-cyclotriphosphazenes (**7** and **8**), respectively, with heterocyclic amines in THF. The new cyclotriphosphazene derivatives were characterized by elemental analysis, FTIR, MS, 1D ^{1}H, ^{13}C and ^{31}P NMR and 2D HSQC, and HMBC techniques. According to the crystallographic data, compound **8** gives rise to an intermolecular hydrogen bond leading to the formation of dimers, and the benzene molecules fill in the cavities between dimerized two cyclotriphosphazene molecules. This situation has strong potential as a supramolecular synthon. On the other hand, the cytotoxic, apoptotic, and necrotic effects of cyclotriphosphazene derivatives in L929 fibroblast and A549 lung cancer cell lines were investigated, which, to best of our knowledge marks, one of the first reports on phosphazene-induced cytotoxicity, apoptosis, and necrosis in these cells. Our results indicated that the toxicity of cyclotriphosphazenes against A549 lung cancer cells was greater than that against L929 fibroblast cells. While only **9a** showed low cytotoxicity in the fibroblast cells, the phosphazenes (**9c**, **10b**, and **10c**) exhibited moderate cytotoxic activity against A549 lung cancer cell lines at 100 µg/mL concentration. While the apoptotic effect of the phosphazenes in L929 fibroblast cells was greater than that in A549 lung cancer cells, the necrotic effect of the compounds was in the opposite order of the cells. In addition, **10a** and **9b** were capable of inducing apoptosis in L929 fibroblast and A549 lung cancer cells, respectively. Phosphazenes **9a** and (**7**, **9b**, and **10b**) caused a necrotic effect in L929 fibroblast and A549 lung cancer cells, respectively. The antibacterial activities of some phosphazenes (**6**–**8**, **10a**, and **10b**) were comparable to or greater than the standards *Ampicillin* and *Chloramphenicol*. Regarding antibacterial activity against *Escherichia coli* 35218, generally the 1,4-ethane diamine precursor for partly substituted **sbs** phosphazenes and the eight-membered *ansa* ring for partly substituted **sas** phosphazenes are important. In the case of heterocyclic amine substituted **sas** phosphazenes, the nine-membered *ansa* ring is especially important, together with a heterocyclic amine substituent. The presence of the nine-membered *ansa* ring instead of the heterocyclic amine type is also an important factor for antifungal activity against *Candida albicans*. Consequently, the antimicrobial activity of the cyclotriphosphazenes depends on the chain length of alkane diamine precursor and whether the substituents bonded to the P-atoms, phosphazene skeleton, and/or compound itself. In the case of the

interaction of phosphazenes with pBR322 plasmid DNA, phosphazene derivatives (**5**, **7**, **8**, **9b**, **9c**, **10a**, and **10b**) were found to be effective in changing the mobility of the DNA. The findings of this study may thus benefit the development of effective applications in medicine such as cancer therapy.

Acknowledgements

The authors express their deep gratitude and heartiest thanks to Ankara University Scientific Research Projects (BAP) (grant no. 10B4240008) and Hacettepe University Scientific Research Unit (grant no. 02 02 602 002) for their financial support of this work.

Appendix A. Supplementary data

HSQC and HMBC spectra of **9b** and **9c**, the crystal packing diagram, and the ring conformations of **8**. The X-ray crystallographic data in CIF format for compound **8** were deposited at the Cambridge Crystallographic Data Center (CCDC), and supplementary crystallographic data can be obtained free of charge upon request at www.ccdc.cam.ac.uk/conts/retrieving.html (or from the director of the CCDC, 12 Union Road, Cambridge CB2 1EZ, UK; fax: +44(0)1223-336033; e-mail: deposit@ccdc.cam.ac.uk, citing CCDC No. 1043941.

References

[1] C. W. Allen, Studies in Inorganic Chemistry; R. Steudel, Ed.; Elsevier: Amsterdam, The Netherlands, 1992; Vol. 14, pp 171–191.

[2] M. Gleria and R. De Jaeger, Phosphazenes: A Worldwide Insight, Nova Science Publishers, Inc., 2004.

[3] B. A. Omotowa, B. S. Phillips, J. S. Zabinski and J. M. Shreeve, *Inorg. Chem.*, 2004, **43,** 5466.

[4] J. Jiménez, A. Laguna, E. Gascón, J. A. Sanz, J. L. Serreno, J. Barberá and L. Oriol, *Chem. Eur. J.*, 2012, **18**, 16801.

[5] L. –J. Qian, L. –J. Ye, G. –Z. Xu, J. Liu and J. –Q. Guo, *Polym. Degrad. Stabil.*, 2011, **96**, 1118.

[6] P. Schroögel, M. Hoping, W. Kowalsky, A. Hunze, G. Wagenblast, C. Lennartz and P. Strohriegl, *Chem. Mater.*, 2011, **23**, 4947.

[7] S. V. Sazhin, M. K. Harrup and K. L. Gering, *J. Power Sources*, 2011, **196**, 3433.

[8] R. K. Voznicová, J. Taraba, J. Příhoda and M. Alberti, *Polyhedron*, 2008, **27**, 2077.

[9] I. Porwolik-Czomperlic, K. Brandt, T. A. Clayton, D. B. Davies, R. J. Eaton and R. A. Shaw, *Inorg. Chem.*, 2002, **41**, 4944.

[10] S. Beşli, S. J. Coles, D. B. Davies, R. J. Eaton, M. B. Hursthouse, A. Kılıç, R. A. Shaw, G. Y. Çiftçi and S. Yeşilot, *J. Am. Chem. Soc.*, 2003, **125**, 4943.

[11] S. Sengupta, *Polyhedron*, 2003, **22**, 1237.

[12] A. Kılıç, S. Begeç, B. Çetinkaya, Z. Kılıç, T. Hökelek, N. Gündüz and M. Yıldız*, Heteroat. Chem.*, 1996, **7**, 249.

[13] M. A. Benson, R. Boomishankar, D. S. Wright and A. Steiner, *J. Organomet. Chem.*, 2007, **692**, 2768.

[14] M. Yıldız, Z. Kılıç and T. Hökelek, *J. Mol. Struct.*, 1999, **510**, 227.

[15] D. Kumar, N. Singh, K. Keshav and A. J. Elias, *Inorg. Chem.*, 2011, **50**, 250.

[16] S. J.Coles, D. B. Davies, R. J. Eaton, M. B. Hursthouse, A. Kılıç, R. A. Shaw and A. Uslu, *Dalton Trans.*, 2006, **10**, 1302.

[17] S. Begeç, *Heteroatom Chem.*, 2007, **18**, 372.

[18] K. Muralidharan and A. J. Elias, *Inorg. Chem.*, 2003, **42**, 7535.

[19] J. O. Bovin, J. Galy, J. F. Labarre and F. Sournies, *J. Mol. Struct.*, 1978, **49**, 421.

[20] I. Porwolik-Czomperlik, M. Siwy, D. Şek, B. Kaczmarczyk, A. Nasulewicz, I. Jaroszewicz, M. Pelczynska and A. Opolski, *Acta Pol. Pharm.*, 2004, **66**, 267.

[21] K. Brandt, T. J. Bartczak, R. Kruszynski and I. Porwolik-Czomperlik, *Inorg. Chim. Acta*, 2001, **322**, 138.

[22] J. L. Sassus, M. Graffeuil, P. Castera and J. F. Labarre, *Inorg. Chim. Acta*, 1985, **108**, 23.

[23] R. Andrews, *IRCS Med. Sci.*, 1979, **7**, 285.

[24] G. Guerch, J. F. Labarre, R. Lahana, R. Roques and F. Sournie, *J. Mol. Struct.*, 1983, **99**, 275.

[25] T. Yıldırım, K. Bilgin, G. Yenilmez Çiftçİ, E. Tanrıverdi Eçik, E. Şenkuytu, Y. Uludağ, L. Tomak and A. Kılıç, *Eur. J. Med. Chem.*, 2012, **52**, 213.

[26] M. Siwy, D. Şęk, B. Kaczmarczyk, I. Jaroszewicz, A. Nasulewicz, M. Pelczyñska, D. Nevozhay and A. Opolski, *J. Med. Chem.*, 2006, **49**, 806.

[27] E. E. İlter, N. Asmafiliz, Z. Kılıç, L. Açık, M. Yavuz, E.B. Bali, A.O. Solak, F. Büyükkaya, H. Dal and T. Hökelek, *Polyhedron*, 2010, **29**, 2933.

[28] A. Natsagdorj, Ph. D. Thesis, 2002, Ankara University, Department of Chemistry.

[29] S. Bilge, Ş. Demiriz, A. Okumuş, Z. Kılıç, B. Tercan, T. Hökelek and O. Büyükgüngör, *Inorg. Chem.*, 2006, **45**, 8755.

[30] S. Bilge, A. Natsagdorj, Ş. Demiriz, N. Çaylak, Z. Kılıç and T. Hökelek, *Helv. Chim. Acta*, 2004, **87**, 2088.

[31] L. J. Farrugia, *J. Appl. Cryst.*, 1997, **30**, 565.

[32] International Tables for X-Ray Crystallography (1974) Vol. IV. Kynoch Press, Birmingham (Present Distributor: Kluwer Academic Publisher, Dordrecht, The Netherlands).

[33] Bruker (2005). SADABS. Bruker AXS Inc. Madison, Wisconsin, USA.

[34] G. M. Sheldrick, SHELXS-97 and SHELXL-97, University of Göttingen, Germany, 1997.

[35] C. Perez, M. Paul and P. Bazerque, *Acta. Bio. Med. Exp.*, 1990, **15**, 113.

[36] A. Okumuş, Z. Kılıç, T. Hökelek, H. Dal, L. Açık, Y. Öner and L. Y. Koç, *Polyhedron*, 2011, **30**, 2896.

[37] H. Cheng, F. Huq, P. Beale and K. Fisher, *Eur. J. Med. Chem.*, 2006, **41**, 896.

[38] Z. M. O. Rzayev, M. Türk and E. A. Söylemez, *Bioorg. Med. Chem.*, 2012, **20**, 5053.

[39] M. Türk, Z. M. O. Rzayev and S. A. Khalilova, *Bioorg. Med. Chem.*, 2010, **18**, 7975.

[40] M. Willson, L. Lafaille, L. Vidaud and J. F. Labarre, *Phosphorus Sulfur*, 1987, **29**, 147.

[41] S. Bilge, B. Özgüç, S. Safran, Ş. Demiriz, H. İşler, M. Hayvalı, Z. Kılıç and T. Hökelek, *J. Mol. Struct.*, 2005, **748**, 101.

[42] D. Cremer and J. A. Pople, *J. Am. Chem. Soc.*, 1975, **97**, 1354.

[43] F. H. Allen, O. Kennard, D. G. Watson, L. Brammer, G. Orpen and R. J. Taylor, *Chem. Soc. Perkin Trans. 2.*, 1987, **12**, 1.

[44] A. B. Chaplin, J. A. Harrison and P. J. Dyson, *Inorg. Chem.*, 2005, **44**, 8407.

[45] G. J. Bullen, *J. Chem. Soc. A*, 1971, 1450.

[46] B. Tercan, T. Hökelek, S. Bilge, A. Natsagdorj, Ş. Demiriz and Z. Kılıç, *Acta Crystallogr.*, 2004, **E60**, o795.

[47] S. Bilge Koçak, S. Koçoğlu, A. Okumuş, Z. Kılıç, A. Öztürk, T. Hökelek, Y. Öner and L. Açık, *Inorg. Chim. Acta*, 2013, **406**, 160.

[48] E. Çil, M. A. Tanyıldızı, F. Özen, M. Boybay, M. Arslan and A. O. Görgülü, *Arch. Pharm. Chem. Life Sci.*, 2012, **345**, 476.

[49] K. Koran, A. Özkaya, F. Özen, E. Çil and M. Arslan, *Res. Chem. Intermed.*, 2013, **39**, 1109.

[50] M. Işıklan, N. Asmafiliz, E. E. Özalp, E. E. İlter, Z. Kılıç, B. Coşut, S. Yeşilot, A. Kılıç, A. Özturk, T. Hökelek, L. Y. Koç Bilir, L. Açık and E. Akyüz, *Inorg. Chem.*, 2010, **49**, 7057.

[51] N. Asmafiliz, Z. Kılıç, A. Öztürk, T. Hökelek, L.Y. Koç, L. Açık, O. Kısa, A. Albay, Z. Üstündağ and A. O. Solak, *Inorg. Chem.*, 2009, **48**, 10102.

[52] N. Asmafiliz, Z. Kılıç, T. Hökelek, L. Açık, L. Y. Koç, Y. Süzen and Y. Öner, *Inorg. Chim. Acta*, 2013, **400**, 250.

[53] Y. Tümer, N. Asmafiliz, Z. Kılıç, T. Hökelek, L. Y. Koç, L. Açık, M. L. Yola, A. O. Solak, Y. Öner, D. Dündar and M. Yavuz, *J. Mol. Struct.*, 2013, **1049**, 112.

Graphical Abstract

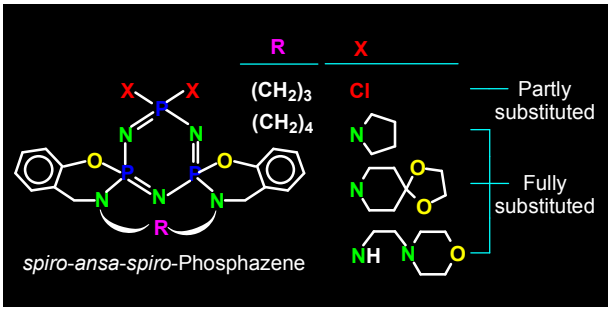

The partly substituted *spiro-ansa-spiro*-cyclotriphosphazenes were reacted with heterocyclic amines to obtain fully substituted cyclotriphosphazenes. The phosphazene derivatives were characterized and investigated for their DNA binding, *in vitro* antimicrobial activities and cytotoxic, apoptotic, and necrotic effects upon L929 fibroblast and A549 lung cancer cells.